

Characterization of individual nanomagnets by the local Hall effect

F.G. Monzon, D.S. Patterson, and M.L. Roukes*
*Condensed Matter Physics 114-36,
California Institute of Technology,
Pasadena, CA 91125 USA*

We describe a straightforward approach to the characterization of *individual* thin-film NiFe ferromagnets, useful from cryogenic to room temperature. The technique is based upon the local Hall effect (LHE), in which strong fringe fields present near the edge of a ferromagnet induce a Hall voltage in a nanoscale semiconducting cross-junction. Hysteresis loops are obtained for individual nanomagnets of widths ranging from 1 μm to less than 100 nm. The LHE is an intrinsically non-perturbative technique, ideal for application to soft ferromagnetic systems. We anticipate that the theoretical sensitivity of this arrangement can rival that of thin-film SQUID susceptometers, with the added benefit that it is simpler and does not require low temperatures.

PACS: 85.70.Kh, 85.80.Jm, 75.70.-i, 85.90.+h

**Corresponding author:* Phone: (626) 395-2916; Fax: (626) 683-9060; roukes@caltech.edu

keywords: magnetometer, susceptometer, micromagnetics, nanomagnet, nonvolatile memory

Characterization and control of the magnetic properties of small ferromagnetic particles become increasingly important as magnetic recording technology strives for higher bit densities and as novel magnetoelectronic devices utilizing GMR, spin-valve, or other phenomena strive for the level of miniaturization and reliability necessary for commercialization. Understanding the dependence of magnetic properties, such as coercivity and hysteresis loop squareness, on sample size and processing is crucial to device improvement. However, measurements on individual nanomagnets are not, in general, straightforward. Arrays of particles are readily measured by commercial SQUID susceptometers, which have sensitivities in the range of 10^{-7} emu, but measurement of submicron-scale particles present a challenge given their small dipole moments. As an example, one would typically need over 2,300 $\text{Ni}_{81}\text{Fe}_{19}$ ($M_s = 850 \text{ emu/cm}^3$) particles of size $1 \mu\text{m}^2 \times 500 \text{ \AA}$ in order to reach the threshold of detectability. Alternatively, one can place single particles in the center of the pick-up coil of a thin-film dc SQUID,^[1] which can provide sensitivity as small as a few thousand Bohr magnetons ($\sim 10^{-17}$ emu). This approach has a much higher level of fabrication complexity and, additionally, requires cryogenic temperatures. Alternative include methods based upon electron microscopy,^[2] including electron holography,^[3] optical techniques based upon the Kerr effect;^[4] and magnetic force microscopy.^[5,6] These are excellent probes of the micromagnetic details of individual particles, but require specialized equipment and, except for the Kerr effect, are often not readily adapted to the exploration of magnetization dynamics in swept fields.^[7] The work we report here complements a previous demonstration of the utility of small Hall probes for characterization of magnetic surfaces, which was demonstrated in a scanning probe arrangement yielding submicron spatial resolution.^[8]

The local Hall effect (LHE) method utilized here requires only standard photo- and electron beam (e-beam) lithographic apparatus, in addition to basic electronics for magnetic field-

dependent measurements. Fig. 1 shows the device configuration. The method is summarized as follows (complete details have been provided elsewhere).^[9] A small ferromagnet (F) is deposited, via a liftoff process, on top of a semiconducting cross-junction so that one edge of F is positioned directly over the center of the cross. A small a.c. bias current is applied to the cross junction while an external in-plane magnetic field is varied. Fringe fields from the edge of F induce an a.c. Hall voltage that is directly proportional to the magnitude and direction of the particle's magnetization. This Hall voltage is then detected with a lock-in amplifier.

The ferromagnets and Hall crosses are patterned using e-beam lithography, which provides alignment accuracy of better than 50 nm. The base pressure before e-beam evaporation of the NiFe magnets is typically better than 5×10^{-7} Torr. Magnets, typically 500 Å thick, are deposited in the presence of a magnetic field oriented along their long axes (this protocol, used to induce a well-defined easy-axis of magnetization, is likely unnecessary for magnets with large aspect ratios). Deposition rates are varied from 1 to 3 Å/s; under these conditions we expect the deposited films to be slightly Ni-poor.^[10] A thin Au layer is always deposited over the magnets in order to prevent oxidation. In some cases for the smallest magnets a thin Ag layer, which seems to promote adhesion, is deposited before the NiFe. Hall crosses are patterned in the underlying n+ GaAs material (carrier density: $n = 10^{18}$ cm⁻³, thickness: 750 Å) by Ar ion milling at 500V.

Important virtues of local Hall sensing are: *a)* it is an extremely *non-perturbative* technique, *b)* it can provide *quantitative* information about local fields, *c)* it is readily applied to *swept-field* measurements, and *d)* it has potential for true *dynamic* measurements. We address these points in turn: *a)* Although improvements in MFM technology have allowed measurements on soft ferromagnetic films with seemingly minimal perturbation,^[5] progressively smaller tips, with

increasingly stronger gradient fields, are required to obtain sufficient resolution for observing the smallest magnetic particles or domains. Coupling between the magnetic tip and sample can then become problematic in that it can perturb domain structure as scans are performed. By contrast, the LHE technique employs no additional magnetic materials, therefore such concerns are eliminated. *b)* In the LHE, the Hall resistance developed is directly proportional to the local field integrated over the cross junction area, hence, with appropriate calibration, it can be employed to extract quantitative information. *c)* Measurements on nanomagnets in swept external fields, H , can be complicated when carried out via MFM or approaches based upon electron microscopy, since the applied field can perturb the measurement apparatus. In the former case, the domain structure of the magnetic tip can be affected by H , whereas in the latter case electron trajectories can be shifted. No analogous issues arise with the LHE; the background Hall signal arising from the presence of a perpendicular component of H can be readily identified and subtracted. *d)* LHE devices can be implemented in geometries providing very large bandwidths--measurements on sub-nanosecond time scales should be attainable through careful high frequency design (e.g. employing leads formed as striplines or coplanar waveguides.)

To demonstrate the remarkable utility of the LHE technique we present a series of measurements made on individual nanomagnets having a range of aspect ratios and widths, in a swept magnetic field, H . Typical data is displayed in the inset of Fig. 2, where the Hall resistance, R_H , from a series of magnets of aspect ratio (AR) ~ 10 manifests hysteretic behavior. This data was obtained at room temperature. Note that these hysteresis loops, R_H vs. H , are controlled by the magnetization near the end of the particle. Accordingly, they directly mirror information about edge domains in this locale, but do not necessarily reveal all the detailed micromagnetics that occur within the entire particle. However, in a long thin magnetic particle

with square or slightly rounded ends, magnetization reversal usually begins at the particle's ends.^[11] Hence the LHE sensitivity to edge domains and the nucleation of vortices can provide valuable insight into switching dynamics in small ferromagnets.

The shape of the hysteresis loops, and the coercivity, H_c , both vary greatly with aspect ratio and width. We display the variation of H_c with magnet width in Fig. 2, for a family of devices with aspect ratio 10. In addition, Fig. 3 presents hysteresis loops for magnets of various aspect ratios, at widths of 500nm, 175nm, and 125nm. Magnets having widths of 500nm or narrower almost always displayed sharp hysteresis loops, with the apparent remanent field, $B_r = B(H_{\text{applied}}=0)$, equal to the saturation field, B_s . Within a family of devices fabricated in the same run, H_c monotonically increased as magnet width decreased. This is in qualitative agreement with the expectation that, as magnetization rotates away from its easy axis, a thinner magnet has a larger magnetostatic energy barrier to overcome. However, as Fig. 2 shows, H_c can vary substantially for magnets of (nominally) identical geometry patterned in different deposition runs, even though conditions were nominally kept identical. Possible sources of this sample-specific variation may include low-level surface contaminants, or edge roughness arising from irregular NiFe liftoff. The latter is a particularly salient issue; the engineering of systematic, tightly-controlled properties in nanomagnets may require exceedingly precise nanofabrication (not our primary focus here), since geometric details on the scale of 10nm may prove relevant in determining edge-domain configurations.^[12]

Hysteresis loops for magnets having different aspect ratios are plotted in Fig. 3. In Fig. 3a data from 500nm wide magnets show that an aspect ratio of at least 5 is needed to obtain a relatively square loop. In Fig. 3b, we display square hysteresis loops for four 175nm wide magnets (all patterned simultaneously on the same chip), even at small aspect ratios ~ 2 . Fig. 3b

also shows that H_c reaches a maximum near an aspect ratio of 5, then decreases with increasing aspect ratio. Similar behavior has been previously reported for Ni and Co magnets (width 100nm), and has been interpreted as evidence for a transition between coherent and incoherent switching dynamics.^[13] Our larger data set, however, suggests the experimental picture is more complicated: we find that magnets fabricated on different chips at different times need *not* show the same local maximum in H_c ; this is demonstrated by the data of Fig. 3c for 125nm wide magnets. Again, this appears to indicate the crucial role that extremely fine scale geometric details play in determining magnetization dynamics. The central point we stress here is that such variation in magnetization dynamics can be readily sensed, in individual nanomagnets, using the LHE.

The temperature dependence of the coercive fields is reflected in our comparison of results obtained at 300 K and 4.2 K, as shown in Fig. 4a. The top pair of hysteresis loops is from a 175nm x 1.75 μ m magnet while the bottom pair is from a 125nm x 5 μ m magnet. Both sets of data show the expected increase in H_c as temperature decreases. The 125nm magnet also shows possible evidence of sequential switching of multiple domains on one side of the hysteresis loop obtained at 4.2 K (the bump between 350 and 400 Oe), although no such indication is found at 300 K. Higher resolution traces in the region of the transition, obtained by decreasing the sweep rate from slightly greater than 2 Oe/s to less than 0.2 Oe/s, are shown in Fig. 4b. At this resolution we can observe evidence for an intermediate magnetization state, indicating that multi-domain behavior sometimes occurs, at least at the edge of the magnet.

Despite the square hysteresis loops of many of our nanomagnets, we generally expect that their magnetization reversal involves multiple domains. Within the literature there exists essentially two definitions of single-domain behavior, static and dynamic.^[13,14] The first is

satisfied if all, *or nearly all*, of a particle's moments align with each other in zero applied field. It is important to note that, for magnetoelectronic devices that employ ferromagnets switched between static remanent states, this static criterion is most relevant — at least from the standpoint of quasi-static device characteristics. Magnets up to a few hundred nanometers in width and thickness can, operationally, satisfy this criterion^[15] depending on the strength of their magnetocrystalline anisotropy (i.e., a larger uniaxial anisotropy allows single-domain properties to be exhibited at a larger size scale). Permalloy has a relatively small anisotropy constant ($K \approx 1500 \text{ ergs/cm}^3$ for 80% Ni)^[16] so is more likely to exist as a multi-domain particle. Nevertheless, our work demonstrates that NiFe particles can still display very square hysteretic behavior at widths of up to a few hundred nanometers. Other factors can assist in yielding square loops: shape anisotropy, deposition in an ambient field (which tends to directionally order the binary alloy), and a favorable exchange constant (which for NiFe is comparable to that of Ni, Fe, and Co). If a magnet is predominantly, but not strictly, single domain, the slight difference between the remanence and saturation magnetization may be virtually unresolvable.

The criterion for *dynamic* single-domain behavior is much more stringent. It requires that moments within a magnetic particle align with each other even as the particle's magnetization reverses; i.e., all moments are required to coherently rotate with one another. This criterion, relevant for macroscopic quantum tunneling experiments,^[14] has been evaluated by fitting experimental switching data to the classical Néel-Brown theory of magnetization reversal. Measurements carried out at temperatures of a few hundred mK show that only particles with diameters of order 30nm, or smaller, show such single domain dynamics.^[14] The NiFe particles explored here are not in this regime. Despite the fact that, at 4.2 K, our smallest magnets often display abrupt transitions (Fig. 4b), we do not interpret this as evidence for coherent switching

for two reasons. First, the local fields that generate our hysteresis loops solely involve magnetization near the end of the particle. For a long thin magnetic particle with square, or slightly rounded ends, magnetization reversal begins at the particle's ends and proceeds then towards the particle's center.^[17] Even for a multi-domain vortex state, the process occurring at the magnet's end might evolve over an extremely small interval of the applied field. Second, once reversal is nucleated at the particle ends, full reversal (over the entire particle) can occur very rapidly, on the scale of nanoseconds.^[18] Hence, lack of coherence in the switching dynamics may be unresolvable without special efforts to increase the temporal resolution of the measurements.

We conclude by considering the ultimate sensitivity of the LHE method. The saturation magnetization density of our NiFe magnets, as determined by SQUID susceptometry measurements on bulk films, is approximately 838 emu/cm^3 . For this value, our LHE measurements on individual $75\text{nm} \times 750\text{nm}$ magnets (thickness 50nm) are indicative of a resolution of $2.36 \times 10^{-12} \text{ emu}$, or $2.54 \times 10^8 \mu_B$ (Bohr magnetons). We expect that much weaker levels of magnetization are detectable. The n+ GaAs cross junctions employed here yield a room temperature Hall coefficient, $dR_H/dH \sim 80 \text{ } \Omega/\text{T}$. Hence at room temperature with a source current of $I_s = 0.5 \text{ mA}$ ^[19] and a room temperature preamplifier with a voltage noise of $V_n = 1 \text{ nV/Hz}^{1/2}$, the ultimate field sensitivity is $B_n^{(\text{rms})} = V_n/I_s \times (dR_H/dH)^{-1} = 2.5 \times 10^{-8} \text{ T/Hz}^{1/2}$. Of course, the efficiency with which a Hall cross can sense the fringe field of a nanomagnet depends upon their relative alignment. Using reasonable estimates for magnet size and geometry, however, one obtains dipole moment sensitivities of just over one hundred Bohr magnetons.^[20]

Geometrical considerations and amplifier noise play important roles in determining the precise value given by such an estimate, but the value obtained above clearly demonstrates that

the local Hall effect is an extremely sensitive probe of magnetization. Further optimization through the use of thinner conducting layers, allowing more effective coupling to strong magnetic fields present near the surface of the cross, should be possible

The spatial resolution of LHE magnetometry is ultimately limited by the smallest junction size attainable, which in turn is determined by edge depletion.^[21] For an n+ electron gas as used here (density $\sim 10^{18} \text{ cm}^{-3}$) this is of order 10 to 20nm (hence the smallest junction area attainable is $\sim 4 \times 10^{-16} \text{ m}^2$).^[22] In techniques such as Kerr or magnetic force microscopy, the ultimate spatial resolution is limited by the size of the laser spot (diffraction limit) or the field profile emanating from the cantilever tip. It is interesting to consider the potential flux sensitivity of ultraminiature LHE devices. A $\sim 4 \times 10^{-16} \text{ m}^2$ Hall junction fabricated in the manner as those reported here, when immersed in a uniform field, will provide a flux sensitivity of $\sim 4 \times 10^{-23} \text{ Wb/Hz}^{1/2}$, i.e. $\sim 2 \times 10^{-8} \phi_0/\text{Hz}^{1/2}$ where $\phi_0 = h/(2e)$ is the flux quantum ($2.07 \times 10^{-15} \text{ Wb}$). Hence *room temperature* performance at the level of state-of-the-art cryogenically-cooled thin film dc SQUIDs appears possible.^[23]

In conclusion, we have shown that the local Hall effect can be an extremely effective method for analyzing the magnetization of small ferromagnetic particles. Experimental optimization of the technique is only in its early stages but the theoretical sensitivity of devices based on the LHE is expected to be comparable to that of on-chip dc SQUID-based susceptometers.^[1,24] Further work is necessary to explore the many possible device applications for LHE devices, the most important of which may be as nonvolatile, radiation-hard, nanoscale memory elements, or as imaging elements for scanned probe (magnetic) microscopy.

We gratefully acknowledge support from the ONR under grant number N00014-96-1-0865.

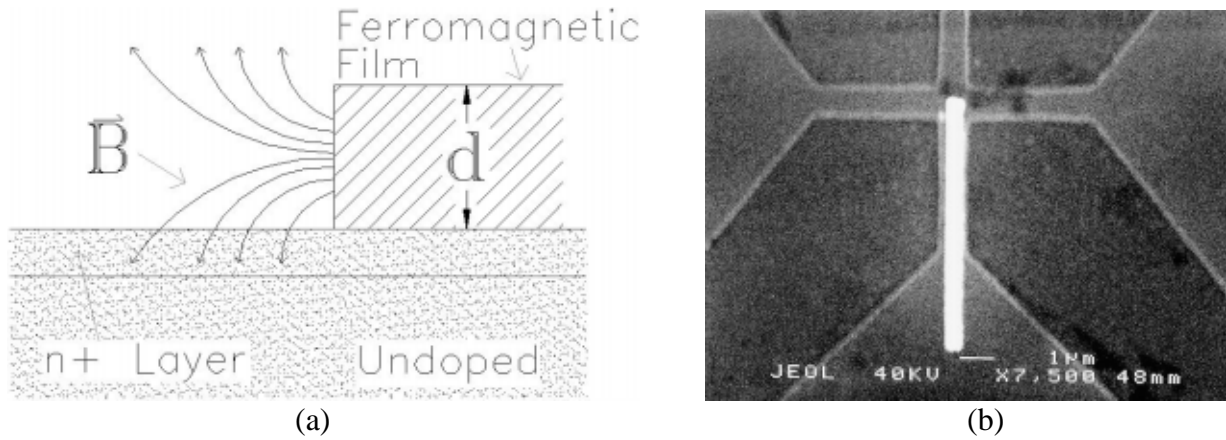


Fig. 1. (a) Schematic side view of a device showing the magnetic fringe field whose perpendicular component, B_{\perp} , induces Hall voltages in the conducting underlayer. The SEM micrograph in (b) shows a NiFe magnet of width 500nm position over a GaAs cross-junction. Magnetization and current flow are directed vertically, while Hall voltage is read out across the horizontal legs.

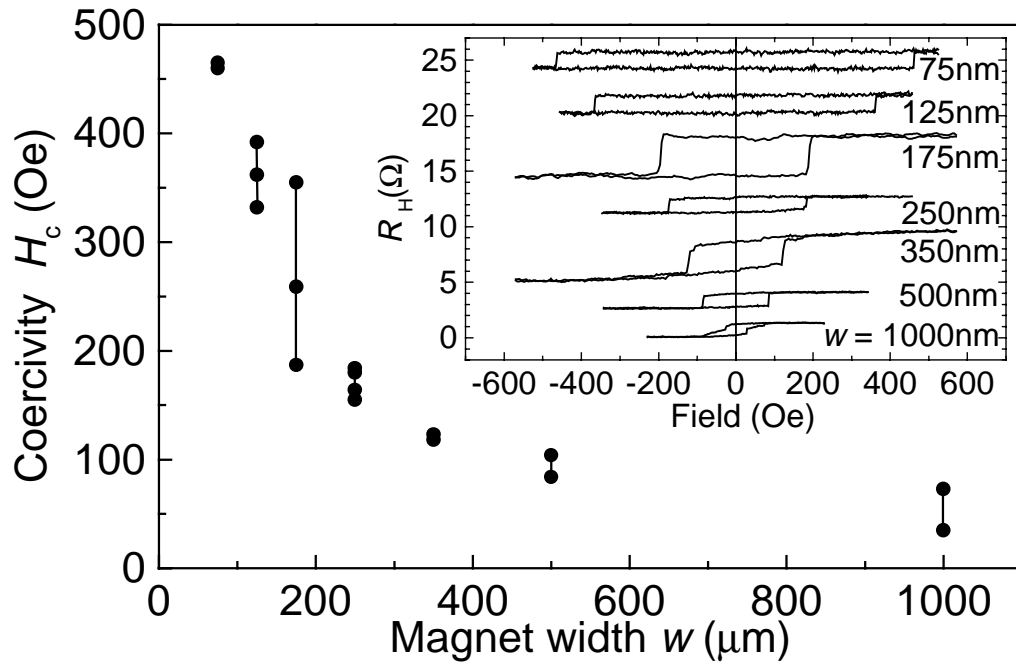


Fig. 2. H_c vs. w for numerous magnets with nominally the same deposition conditions and with aspect ratios of 10. All data were taken at room temperature. Vertical lines connect data points from magnets of the same width. *Inset:* A series of hysteresis loops for magnets of aspect ratio 10, but with varying widths. Traces are offset vertically.

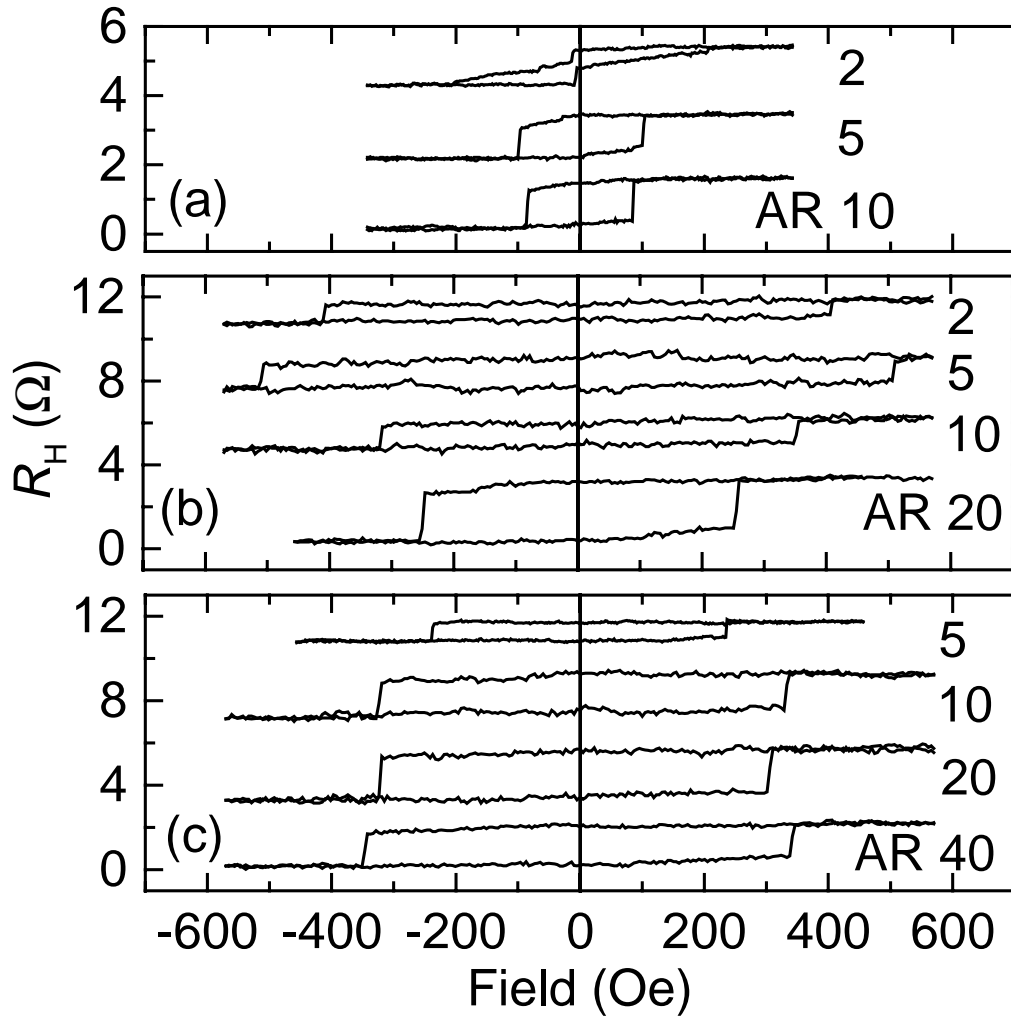


Fig. 3. Hysteresis loops, at 300 K, for different aspect ratio (AR) magnets at the same width. Magnets in (a) are 500nm wide, in (b) are 175nm wide, and in (c) are 125nm wide. Traces are offset vertically.

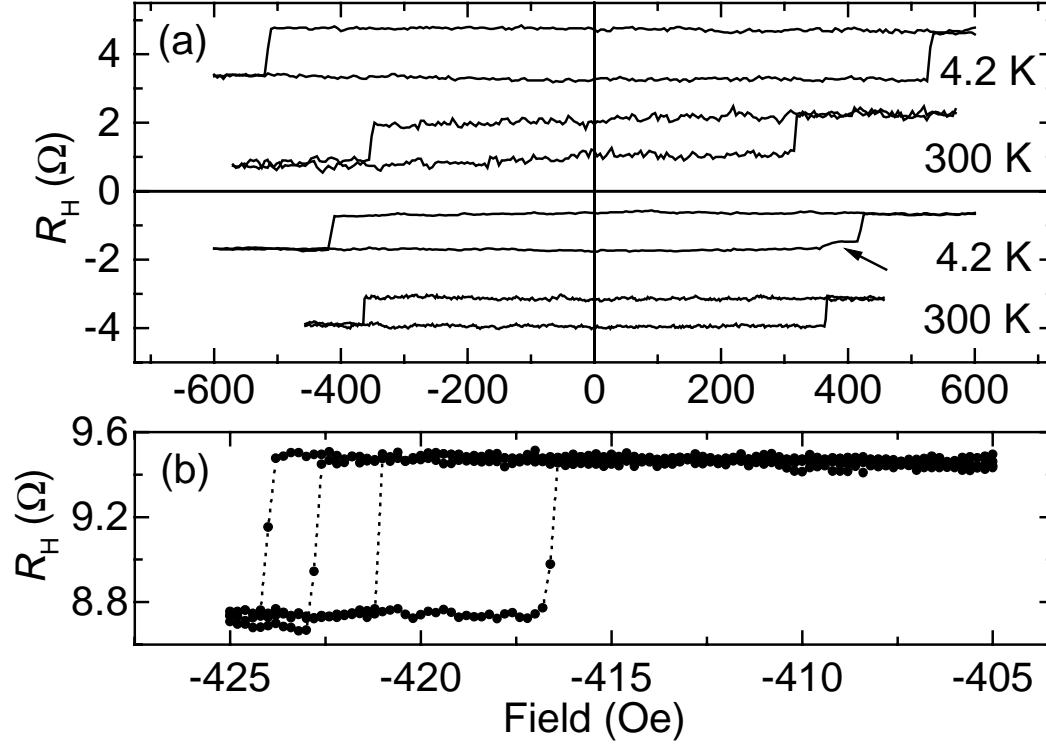


Fig. 4. (a) Hysteresis loops for $175\text{nm} \times 1.75\mu\text{m}$ (top pair) and $125\text{nm} \times 5\mu\text{m}$ (bottom pair) magnets. Despite the large AR of the 125nm magnet, at 4.2 K it displays evidence for incoherent switching (indicated by the arrow). Hysteresis loops are offset for clarity. (b) An enlargement of the transition region of this 125nm magnet, on the side that looks sharp in (a), shows that the transition occurs over a very narrow field range. Our field resolution was 0.1 Oe, and the sweep rate was less than 0.2 Oe/s. Note the spread in coercivity. The vertical offset here was due to lithographic mismatch in the legs of the Hall cross.

-
- ¹ M.B. Ketchen, D.D. Awschalom, W.J. Gallagher, A.W. Kleinsasser, R.L. Sandstrom, J.R. Rozen, and B. Bumble, *IEEE Trans. Magn.* **25**, 1212 (1989).
- ² M.R. Scheinfein, J. Unguris, D.T. Pierce, and R.J. Celotta, *J. Appl. Phys.* **67**, 5932 (1990).
- ³ Akira Tonomura, *IEEE Trans. Magn.* **29**, 2488 (1993).
- ⁴ J. Unguris, R.J. Celotta, and D.T. Pierce, *Phys. Rev. Lett.* **79**, 2734 (1997).
- ⁵ G.A. Gibson and S. Schultz, *J. Appl. Phys.* **73**, 4516 (1993).
- ⁶ Paul B. Fischer, Mark S. Wei, and Stephen Y. Chou, *J. Vac. Sci. Technol. B* **11**, 2570 (1993).
- ⁷ However, new swept, high-field techniques have recently been developed for MFM; see, e.g. Roger Proksch, Erik Runge, Paul K. Hansma, Seryl Foss, and Brian Walsh, *J. Appl. Phys.* **78**, 3303 (1995).
- ⁸ A.M. Chang, H.D. Hallen, L. Harriott, H.F. Hess, H.L. Kao, J. Kwo, R.E. Miller, R. Wolfe, and J. Vanderziel, *Appl. Phys. Lett.* **61**, 1974 (1992).
- ⁹ F.G. Monzon, Mark Johnson, and M.L. Roukes, *Appl. Phys. Lett.* **71**, 3087 (1997).
- ¹⁰ K.R. Carson and M.L. Rudee, *J. Vac. Sci. Technol.* **7**, 573 (1970).
- ¹¹ Youfeng Zheng and Jian-Gang Zhu, *J. Appl. Phys.* **81**, 5471 (1997).
- ¹² Jian-Gang Zhu, Youfeng Zheng, and Xiangdong Lin, *J. Appl. Phys.* **81**, 4336 (1997); and J.-G. Zhu, personal communication.
- ¹³ Linshu Kong and Stephen Y. Chou, *J. Appl. Phys.* **80**, 5205 (1996): A coherently switched magnet's coercivity would increase monotonically with increasing shape anisotropy. However, longer magnets must overcome a larger magnetostatic energy barrier when switching than short magnets. Thus at the same aspect ratio, longer magnets are more likely to switch by means of nucleation of vortices, decreasing the coercivity. See also M.E. Schabes, *J. Magn. Magn. Mater.* **95**, 249 (1991). Vortex states differ from essentially single domain states, such as the "flower"

state of Schabes.

¹⁴ W. Wernsdorfer, E. Bonet Orozco, K. Hasselbach, A. Benoit, D. Maily, O. Kubo, H. Nakano, and B. Barbara, *Phys. Rev. Lett.* **79**, 4014 (1997).

¹⁵ The critical size for static single-domain behavior is sometimes estimated to be approximately the thickness of a domain wall, or less than 100nm in Ni or Fe. However, apparently “single-domain” behavior has been reported by several groups at larger sizes (see ref. 13) and indicates that for practical purposes one can often go to several hundred nanometers in width and still have very square hysteresis loops, especially at 300 K.

¹⁶ This decreases with decreasing Ni fraction until it passes through zero at 75% Ni. See, e.g., B.D. Cullity, *Introduction to Magnetic Materials* (Addison-Wesley, Reading, Massachusetts), pg. 526 (1972).

¹⁷ M.R. Freeman, W.K. Hiebert, and A. Stankiewicz, *J. Appl. Phys.* **83**, 6217 (1998).

¹⁸ S.E. Russek, J.O. Oti, Shehzaad Kaka, and Eugene Y. Chen, *J. Mag. Mag. Mat.*, *to be published*.

¹⁹ This level of current is chosen because it corresponds to modest (\sim few mW) dissipation in a small device and a reasonable voltage drop across the device. (The typical series resistance of a device is 10 k Ω , so the resulting voltage drop is of order 5 V.)

²⁰ The optimal configuration is a thin disk ferromagnet of lateral dimensions slightly bigger than the cross-junction (to provide relatively uniform field through the cross), situated directly above it, with magnetization perpendicular to the junction plane. We thus assume a junction with electrically active area of radius 100nm (similar to the smaller crosses discussed in these experiments) underneath a disk whose magnetization induces a field change of 10^{-7} T through the cross (somewhat above the minimum field sensitivity). The equivalent magnetic moment is then

given by $(\Delta B \times V) / (4\pi - N_d)$ where ΔB is the field change, V is the particle volume, and N_d , the demagnetization factor, is $4\pi[1 - (\pi/2)(t/r)]$ for a thin (t/r small) disk of thickness t and radius r . With $r = 200$ nm (thickness drops out of the calculation) we then obtain a dipole sensitivity of 1.27×10^{-18} emu, or $140 \mu_B$. Though geometry-dependent, this estimate is useful in gauging the high level of sensitivity of the LHE method.

²¹ K.K Choi, D.C. Tsui, K. Alavi, Appl. Phys. Lett. **50**, 110 (1987).

²² Although a larger Hall coefficient would result from use of a lower density electron gas, the depletion width increases and, hence, spatial resolution is degraded.

²³ D.D. Awschalom, J.R. Rozen, M.B. Ketchen, W.J. Gallagher, A.W. Kleinsasser, R.L. Sandstrom, and B. Bumble, Appl. Phys. Lett. **53**, 2108 (1988).

²⁴ W. Wernsdorfer, B. Doudin, D. Maily, K. Hasselbach, A. Benoit, J. Meier, J.-Ph. Ansermet, and B. Barbara, Phys. Rev. Lett. **77**, 1873 (1996).